PROCEEDINGS, 44th Workshop on Geothermal Reservoir Engineering
Stanford University, Stanford, California, February 11-13, 2019
SGP-TR-214

Processing of magnetotelluric data for monitoring changes in electric resistivity during drilling operation

Nadine Haaf[1,2], Eva Schill[1,2]

Karlsruhe Institute of Technology, Hermann-von-Helmholtz-Platz 1, 76344 Eggenstein-Leopoldshafen, Germany

Institute of Applied Geoscience, Technische Universität Darmstadt, Schnittspahnstraße 9,64287 Darmstadt, Germany

nadine.haaf@kit.edu

Keywords: Magnetotellurics, Monitoring, DEEPEGS

1. ABSTRACT

Long-term magnetotelluric monitoring of different injection and production experiments at the Rittershoffen geothermal site in Alsace (France) provided a first continuous data set over several month, covering the end of drilling phase of GRT2 (Abdelfettah et al. 2018), mostly, production from, but also injection into this well, injection into GRT1 and a circulation experiment. Transfer functions showed particular variation pattern for different operations, i.e. an increase in uncertainty, conductivity and phase during test operation with a preferential direction sub-parallel to Shmin, i.e. perpendicular to the expected extension of the fractures controlling the reservoir. In particular fluid injection, either into GRT2 or GRT1 causes a strong decrease in resistivity by up to one order of magnitude in the YX component between about 8–25 s of period. Here, we present particularities of processing of continuous magnetotelluric monitoring for the example of deepening of the RN-15 well on the Reykjanes peninsular (Iceland) to 4665m (IDDP-2 well) with a magnetotelluric dataset from November 2016 to January 2017. The drilling progress during this period was accompanied by partial and up to total circulation loss (Friðleifsson et al. 2017). Two continuous running MT stations, GUN and RAH, were installed on the Reykjanes peninsula. RAH and GUN are located about 6 and 1 km away from IDDP-2. Both MT stations are equipped with two electric dipoles in N-S and E-W direction, as well as three magnetic sensors oriented in N, E and vertical direction. MT monitoring was carried out with a sampling frequency of 512 Hz. Processing revealed the bad data quality of RAH. Consequently, MT data were processed using single site method with the code Bounded Influence Remote Reference Processing (Chave and Thomson 2004). Due to a temporally noise signal in the time series, they were down filtered to get the lower frequency bands and hence to clean the time series. Additionally, a remote station from Germany has been tested to improve the data quality in the dead band. First results might suggest a temporal correlation between low resistivity in the MT data, fluid loss, and induced seismicity.

2. INTRODUCTION

An increasing interest in magnetotelluric (MT) monitoring of hydraulic stimulation experiments results from soft stimulation techniques that reduce induced seismicity to a minimum. MT is a passive electromagnetic method that records the ambient electric and magnetic field to gain information about the electric conductivity of the subsurface. Used for monitoring, the directional evolution of the reservoir, e.g., during reservoir engineering, can be traced.

MT monitoring proved to be useful to trace the directional development of the Paralana and Cooper basin reservoirs during massive hydraulic stimulation experiments by relative phase tensor changes (Peacock et al. 2012; Peacock et al. 2013; Didana et al. 2017). In these experiments, volumes of 3100 m³ and 36,500 m³ were injected at up to 60 L/s and 53 L/s resulting in resulting in reservoir pressures of up to 62 MPa and 48 MPa in the wells Paralana-2 and Habanero-4, respectively. Long-term magnetotelluric monitoring of different low-volume and -pressure injection and production experiments at the Rittershoffen geothermal site in Alsace (France) provided a first continuous data set over several month, covering the end of drilling phase of GRT2 as well as production and injection into both wells GRT1 and 2 (Abdelfettah et al. 2018). Transfer functions showed operation dependent variation, i.e. variation in uncertainty, conductivity and phase with a preferential direction sub-parallel to Shmin, i.e. perpendicular to the expected extension of the fractures controlling the reservoir. In particular fluid injection, either into GRT2 or GRT1 causes a strong decrease in resistivity by up to one order of magnitude in the YX component between about 8–25 s of period.

Similar long-term monitoring during deepening from 2500 to 4659m and development of the RN-15/IDDP-2 well on the Reykjanes peninsular (Iceland) was carried out from November 2016 to January 2017. In this well, the H2020 project DEEPEGS (https://deepegs.eu) aims at demonstrating advanced engineering technologies. A deep Enhanced Geothermal System at Reykjanes aims injection of fluid underneath the conventional geothermal field to support production. The drilling from August 2016 until January 2017 was accompanied by partial and up to total circulation loss. Earlier MT exploration in the area reveals a typical resistivity structure of a high temperature geothermal system with a low resistive cap layer, here, with up to 2 km thickness. In the vicinity of the well vertical conductive structures hint to a dyke swarm or a sheeted dyke complex as heat source (Friðleifsson et al. 2014).

Besides anthropogenic noise, the challenge of processing continuous MT monitoring data are the relatively high-frequency changes in the "perturbed" MT signal. Perturbation in the reservoir are caused during drilling by partial and up to total circulation loss and induced seismicity (Friðleifsson et al. 2017). Here, we present the necessary processing procedure and first results from the final drilling phase.

3. FIELD SURVEY

In a first field campaign in September 2016, eight stations were tested to identify an optimal location for continuous MT monitoring with respect to the expected electric noise (Darnet et al. 2018). During this period a temporary remote station was operated in the region Höfuðborgarsvæðið, 20 km South of Reykjavik. This remote station cannot be accessed during the winter period, when the target depth was reached and main stimulation of the well occurred. For practical operation and maintenance regarding power supply and data transfer and for reasons of data comparability, the two continuous monitoring stations, GUN and RAH, were selected close to seismic stations (Figure 3.1). The GUN station represents the main monitoring site and is located about 750 m SE of the wellhead of RN-15/IDDP-2 well and beeline about 1 km to the E of the bottom of the well the away from the well. The MT station, RAH, is located at about 5 km to the NE. RAH was planned to operate as a second continuous monitoring station with the potential of being a local remote reference.

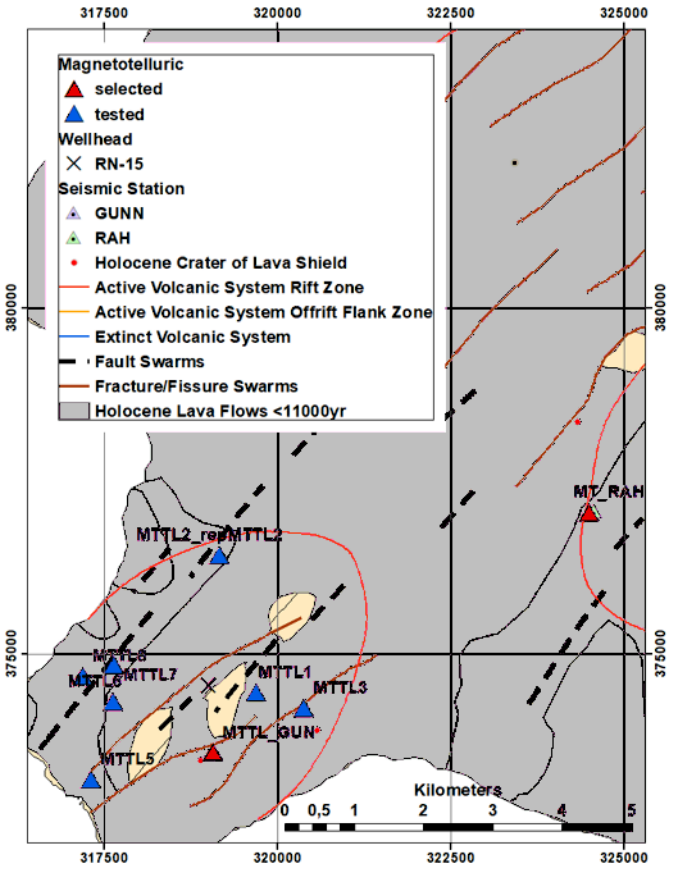

Figure 3.1 Geological map of the Reykjanes peninsular with the MT test (blue triangles) and monitoring stations (red triangles) and the Wellhead of RN15 (black cross).

Both stations were installed with a controlling unit ADU07e from Metronix Inc. to measure orthogonal and time dependent components of the Earth's magnetic field and the corresponding electric response. The so-called time series were measured by two horizontal electric components, E_x and E_y, and three magnetic components, H_x, H_y and H_z. The three MFS07e coils were aligned perpendicular in north-south, east-west and vertical direction, respectively. The electric horizontal dipoles were aligned with the horizontal magnetic coils in N-S and E-W direction. The stations and the cables were buried to about 10 cm depth protect them from the weather.

At GUN, continuous monitoring was carried out between November 30th, 2016 and July 21st, 2017. The sampling frequency was 512 Hz and it was measured in 24-hour blocks. Measurements at RAH were stopped in May 2017 due to continuing bad data quality after mid of December 2016. The MT monitoring covers the last third of the drilling period of the RN-15/IDDP-2 well and the successive stimulation of the well.

4. PROCESSING AND DISCUSSION OF MT DATA

The processing of MT data is carried out using the bounded influence remote reference code ,birrp, (Chave and Thomson 2004) to process the data. Remote referencing is included in the advanced mode of birrp.

4.1 Types of noise and perturbation

Figure 4.1 reveals different types of noise. To better visualize the noise peaks in the spectrum, the power spectral density was calculated and the whole window length is shown. Most prominent peaks appear in all five channels were observed at 14 Hz for the time period between November 30th and 18th, 2016 and 50 Hz and harmonics across the entire monitoring period. This 14 Hz noise signal occurs roughly every 30 minutes with a duration of about 90s. The source of noise could not be identified.

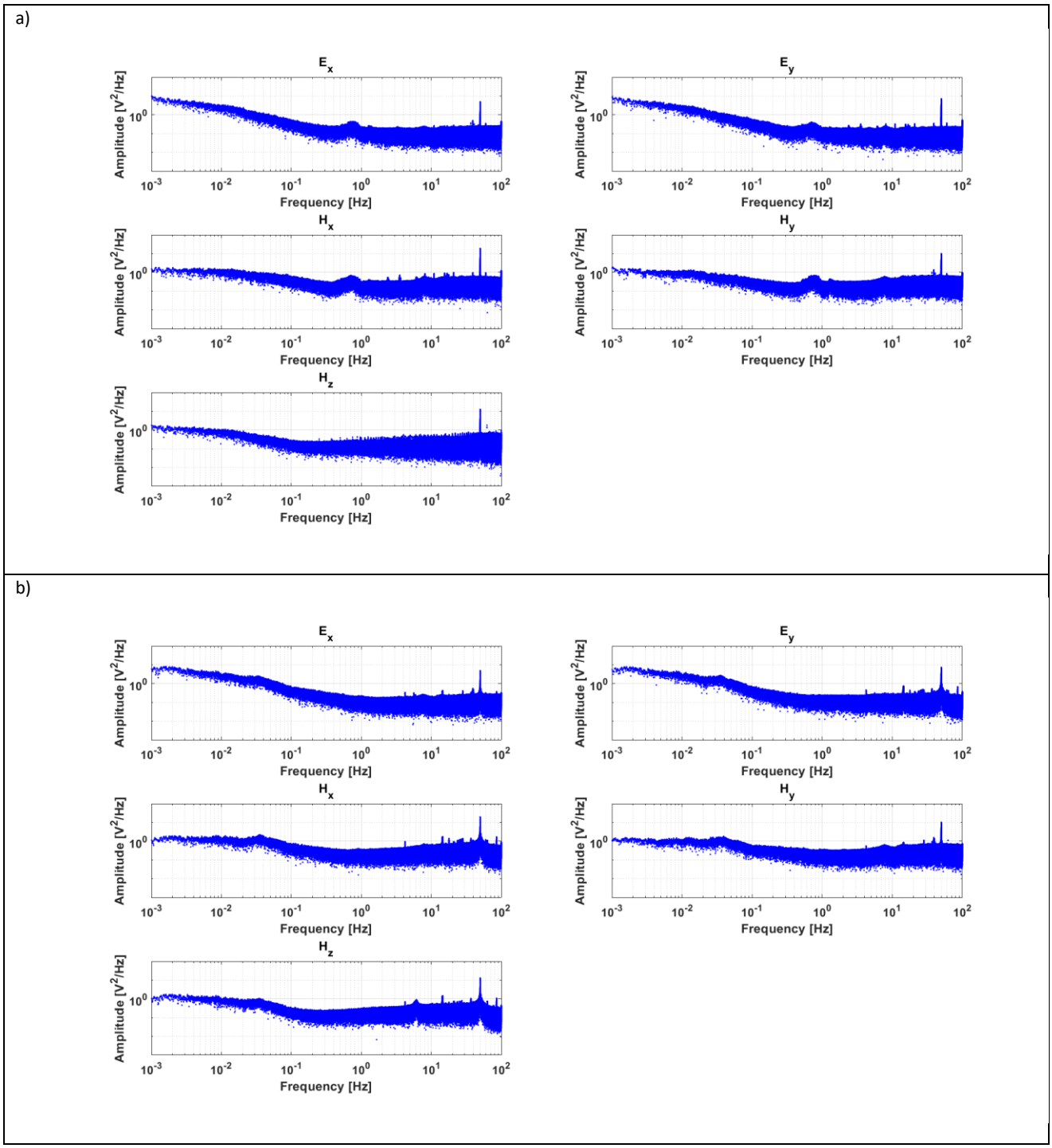

Figure 4.1 Noise spectra in the five channels from a) January 13th, 2017 and b) December 11th, 2016 (decimated to 128 Hz) of GUN MT station.

In the following, we introduce that variability of the single-site processed transfer functions (calculated for 48 h) over the time period of November 30th, 2016 to December 1st, 2016 at the GUN station (Figure 4.2). Typically, temporal variations in electric resistivity occurs between 10^{-1} and 10 s. Changes in the phase are not observed. One end-member type shows apparent resistivities down to about 10^{-1} Ωm at periods of a few tens of seconds (Figure 4.2a). The opposite end-member type reveals apparent resistivities down to 1 Ωm at periods up to 10 s (Figure 4.2b). Note that such decrease in resistivity has been attribute in other geothermal projects such as Rittershoffen (France) to fluid injection (Abdelfettah et al. 2018).

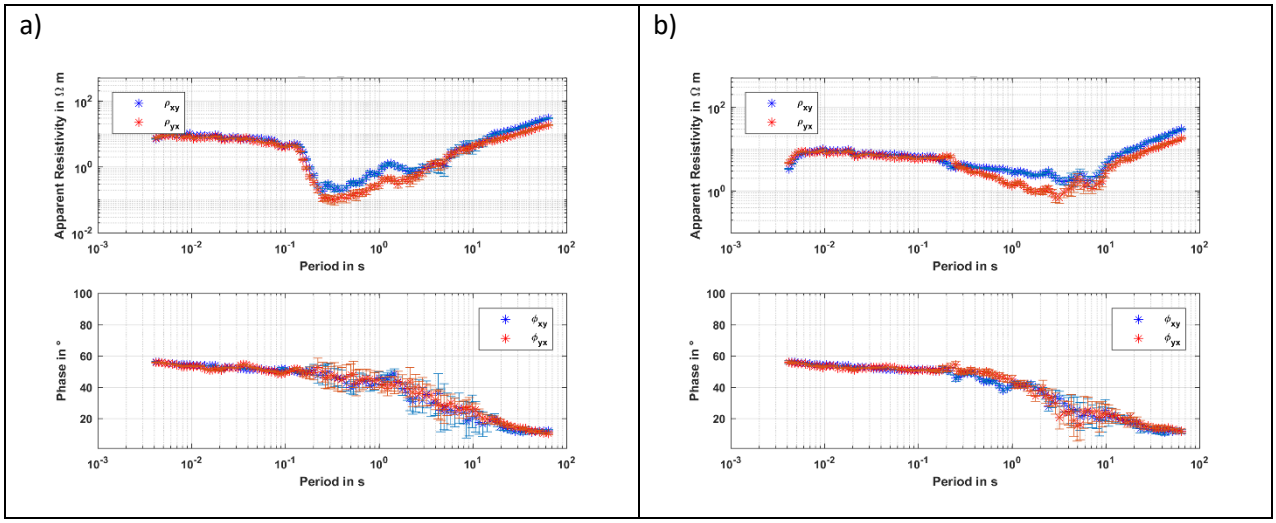

Figure 4.2 Representative end-member types of transfer functions (top: apparent resistivity, bottom phase) with a) a resistivity low (>10^{-1} Ωm) at periods of a few tens of seconds from December 18th to 19th, 2016 and b) a resistivity low (>1 Ωm) at periods of up to 10 s from November 30th to December 1st, 2016.

4.2 Remote Referencing

Following the approaches of Gamble and Clark (CLARKE et al. 1983; GAMBLE et al. 1979) uncorrelated noise can be eliminated from the measured data using remote referencing, when a high degree of correlation between the naturally-induced electromagnetic fields at local and remote site is reached. Thus, the remote reference must be sufficiently distant to the local station, i.e. a few skin depths (Chave et al. 2012), to ensure possible bias errors due to correlated noises to be small compared to the random errors (Chave et al. 2012; GAMBLE et al. 1979).

Note that for MT monitoring the period of the perturbation is crucial for the applicability of remote referencing. Perturbations at the well bottom are caused by changes in the engineering process, i.e. changes in flow rate, pressure or even related seismicity. If of low period with respect to the measurement period and causing an electromagnetic signal, these changes may contribute to uncorrelated noise. Thus, when applying conventional remote referencing, this signal of interest may be weakened or eliminated. For this reason, several remote stations were tested during the project period, a temporary remote reference for the test measurements in September 2016, the RAH station at a distance of 5 km from the drilling platform and the Wittstock remote site in the Northwest of the federal state Brandenburg in Germany. Since the coherency needs to be high for the remote referencing, the transfer functions are averaged over 48 hours to obtain a reasonable resolution for the depth of investigation.

4.2.1 Remote referencing with the temporary remote station

In the following, transfer functions calculated over a period of 48 h from September 25th to 26th, 2016 are discussed. The following operations were carried out at the drilling site during these two days. On September 25th, the loss zones in the well were cemented down to 2950 m with mainly with flow rates of 15 and up to 30 L/s. At 3:10 p.m., a seismic event of magnitude 0.86 occurred in the reservoir zone. On September 26th, drilling was performed from 2945-2950 m with flow rates up to 45 L/s and high frequency changes (Figure 4.3).

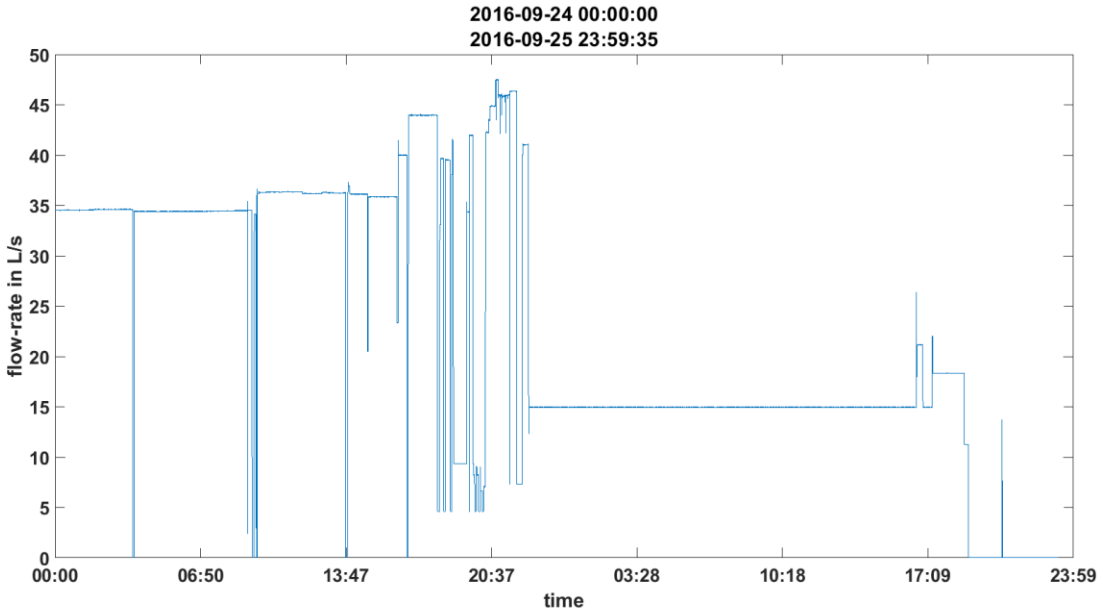

Figure 4.3 Changes in injection flow rate during cementation and drilling from September 25th to 26th, 2016 at the RN15/IDDP2 well.

The single-site processed transfer function of the temporary remote station from September 25th to 26th, 2016 is given in Figure 4.4. Differences in XY and YX components in both apparent resistivity and phase are relatively small indicating a well-layered 1-D underground. Relatively large error bars in the phase between 2 and 10 s reveal some issue of this station being used as remote reference.

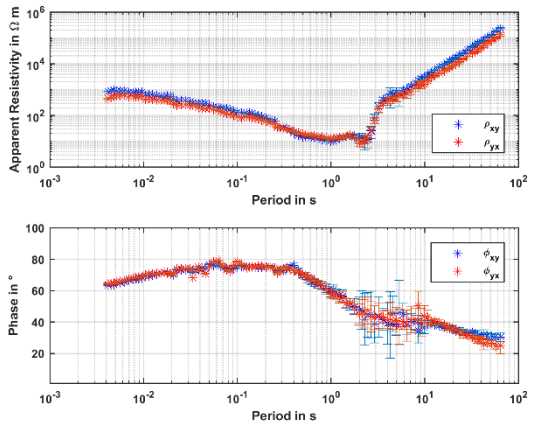

Figure 4.4 Single site processed XY (blue) and YX (red) components of apparent resistivity (a) and phase (b) of the temporary remote reference MT station from September 25th to 26th, 2016.

Figure 4.5 compares the transfer function of the same date using single-site and remote referenced processing. Single-site processing shows comparably small error bars and relatively smooth changes in resistivity and phase over most of the periods. Small outliers are observed at $2.5 \cdot 10^{-1}$ and 1 s in the apparent resistivity and at 1 and 2.5 s in the phase. Between $1.5 \cdot 10^{-1}$ and 1 s the resistivity of the YX component decreases from about 6 Ωm down to 1 Ωm compared >2 Ωm in the XY component. Both, the small outliers and the decrease in resistivity disappear with remote referenced processing. A clear decline in quality of the transfer function is observed for the low periods down to $3 \cdot 10^{-2}$ s.

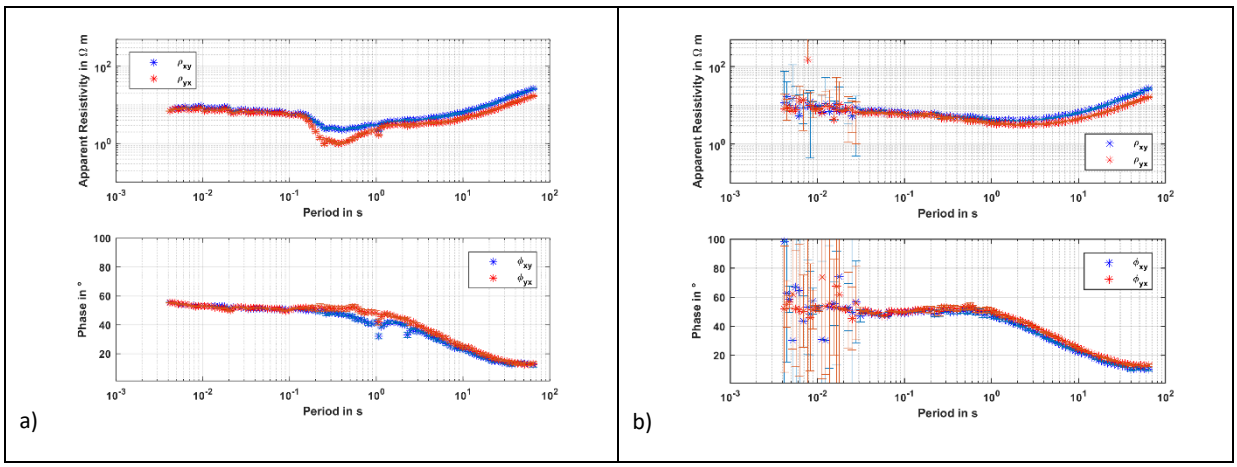

Figure 4.5 a) Single-site and b) remote reference processed transfer functions using the temporary reference station, XY (blue) and YX (red) components of apparent resistivity (top) and phase (bottom) of GUN MT station from September 25th to 26th, 2016.

4.2.2 Remote referencing with the RAH station

For completeness, we present here (Figure 4.6) the remote-referenced transfer functions of the GUN station from January 10th to 11th, 2017 using the RAH station. As mentioned above, these measurements of this station were of bad quality and consequently, the obtained transfer functions reveal unrealistic results ranging from apparent resistivity values of 10^{-6} to 10^{4} Ωm and extreme error bars for the phase.

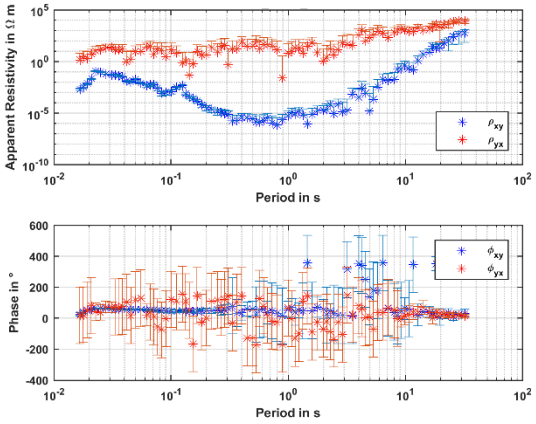

Figure 4.6 Remote reference processed transfer functions using the RAH reference station, XY (blue) and YX (red) components of apparent resistivity (top) and phase (bottom) of GUN MT station from January 10th to 11th, 2017.

4.2.3 Remote referencing with the Wittstock station

The Wittstock station is located in the Northwest of the federal state Brandenburg in the Northeast of Germany and operated by the Geo Research Center, GFZ since 2010 as continuous MT reference station. It is equipped with different sensors to measure both, middle to high frequency variations of the horizontal magnetic field components as well as slow magnetic variations, at sampling rates of 1 Hz to 6 kHz (Ritter et al. 2015a; Ritter et al. 2015b). Representative time series of the horizontal magnetic components of Wittstock from December 11th 2016 are compared in Figure 4.7 to the measurements of the GUN monitoring station revealing specific noise in the period between November 30th to December 18th 2016. In the latter, peaks are observed regularly in the H_x component. Its baseline, however, reveals a smaller amplitude compared to the data from Wittstock. Here, random noise is observed in in both channels.

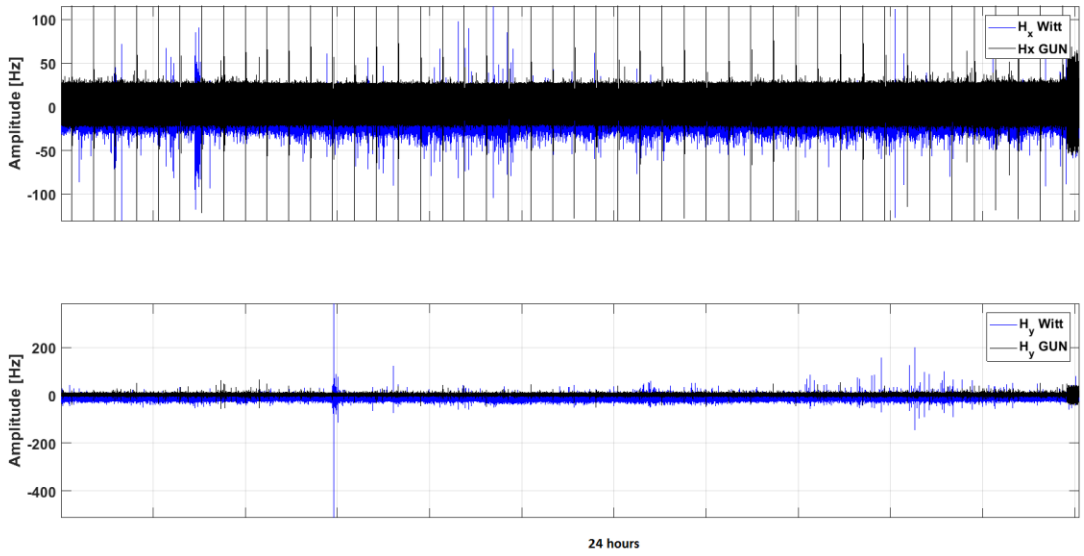

Figure 4.7 Horizontal magnetic components Hx and Hy of representative time series of December 11th 2016 from the Wittstock remote station (black) and the GUN monitoring station (blue).

Due to different sampling frequencies of 250 Hz in Wittstock, compared to 512 Hz at GUN, the data of Wittstock were resampled using interpolation. In Figure 4.8 **Error! Reference source not found.**a comparison between single site and remote referencing processed transfer functions of a representative example from December 17th to 18th 2016 that is comparable to the sample in Figure 4.5 is shown. The single-site processed transfer function reveals low error bars across the entire period range, including the anomaly observed between about 0.2 and 1 s that is pronounced in the YX component of the apparent resistivity. The anomaly disappears in the remote referenced transfer function, leading, however, to a strong increase in error bars at periods > 0.2 s and <0.008 s in both, apparent resistivity and phase.

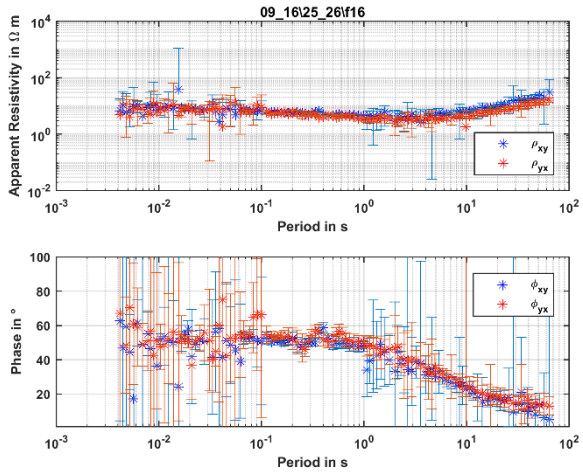

Figure 4.8 Remote reference processed transfer functions using the Wittstock reference station, XY (blue) and YX (red) components of apparent resistivity (top) and phase (bottom) of GUN MT station from September 25th to 26th, 2016.

Given short wavelength of the perturbations introduced by drilling and reservoir engineering (

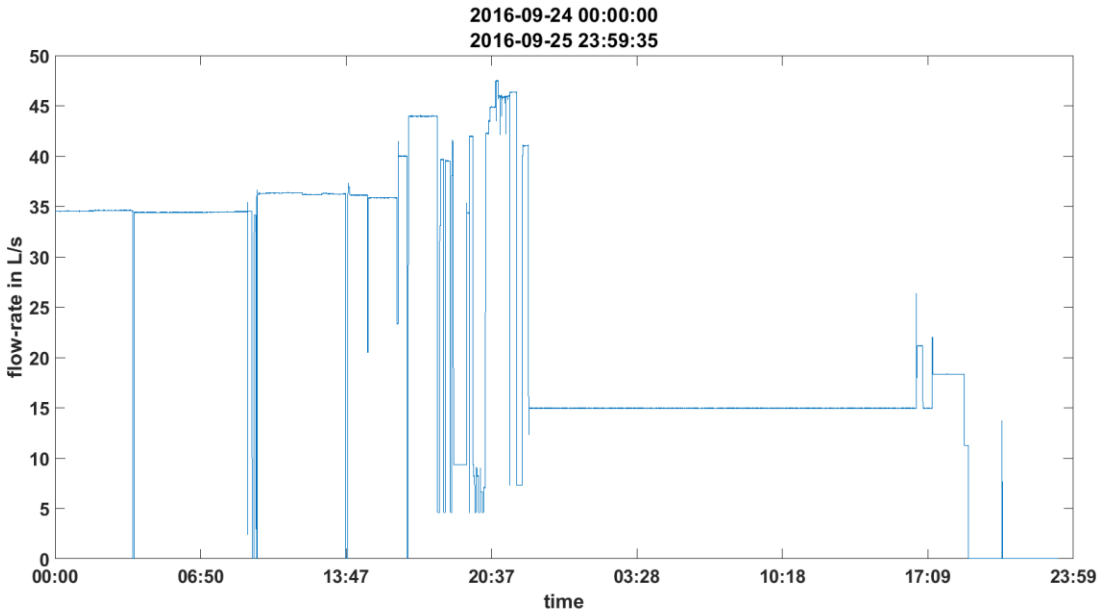

Figure 4.3) as well as even shorter wavelength of seismicity with respect to the period of integration of 48 h, we can consider the sought-after electromagnetic appearing as uncorrelated signal with the distant remote reference station. As shown in Figure 4.6, the local station RAH is not applicable for remote referencing due to bad quality. Thus, in the following, we will address the elimination of noise from the measured data without eliminating the sought-after electromagnetic signal from the introduced perturbations.

4.3 Noise sources

Anthropogenic electromagnetic noise may result from many sources that are often difficult to identify and may occur at significant distance. In Figure 4.9, we present parameters over time that indirectly indicate major possible sources of electromagnetic noise that can arise from activities on the drilling platform, i.e. the pump rates of the three pumps used for mud circulation during drilling, the drill bit's torque, the number of rotations, and the rate of penetration of the drill bit. The torque is the rotational force between the drill string and the formation. The rounds per minute is the frequency of rotations performed by the drill bit whereas the rate of penetration is a measure of the speed at which the drill bit can break the rock under it and thus deepen the wellbore. The drill bit parameters are mainly active until end of December 2016 and then shortly again before end of drilling. In addition, high frequency changes in amplitude are shown in Figure 4.9 for certain time intervals.

In the following, the correlation between changes in the apparent resistivity in the frequency range of interest and these drilling parameters is analyzed. Representative examples for the resistivities of 5 and 10 Hz are shown Figure 4.10 for both polarizations, XY and YX. These frequencies are in the interval between 0.1-4 s, in which significant changes in the transfer functions were observed. Correlation coefficients between the drilling parameters and the resistivities range between 0.27 and 0.5 indicate no correlation. Note that it is not excluded that other sources influence the signal. However, an influence of the operations at surface seem not to be responsible for the resistivity changes in the investigated frequency range.

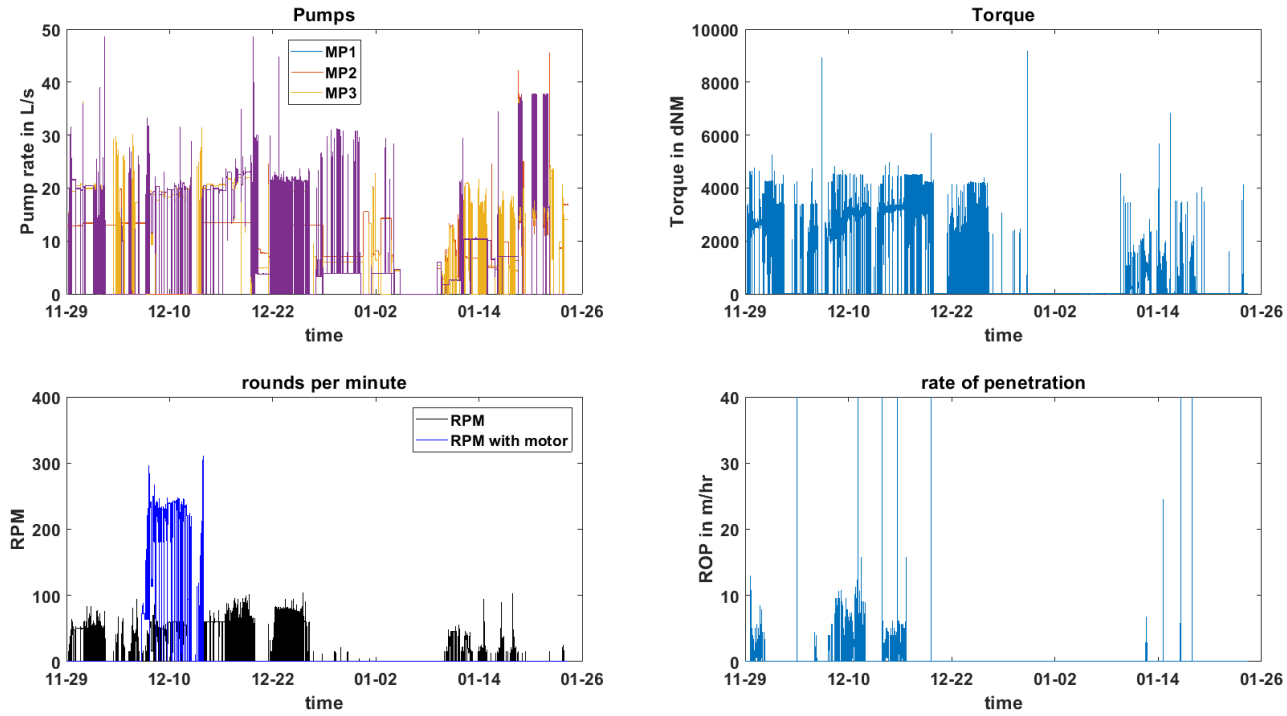

Figure 4.9: Drilling parameters versus time during the final drilling periods: the pump rates of the three pumps on site (left top), number of rotations (rounds per minutes RMP, left bottom), torque (deci-Newton meter, right top), and rate of penetration (meters per hour, right bottom) of the drill bit.

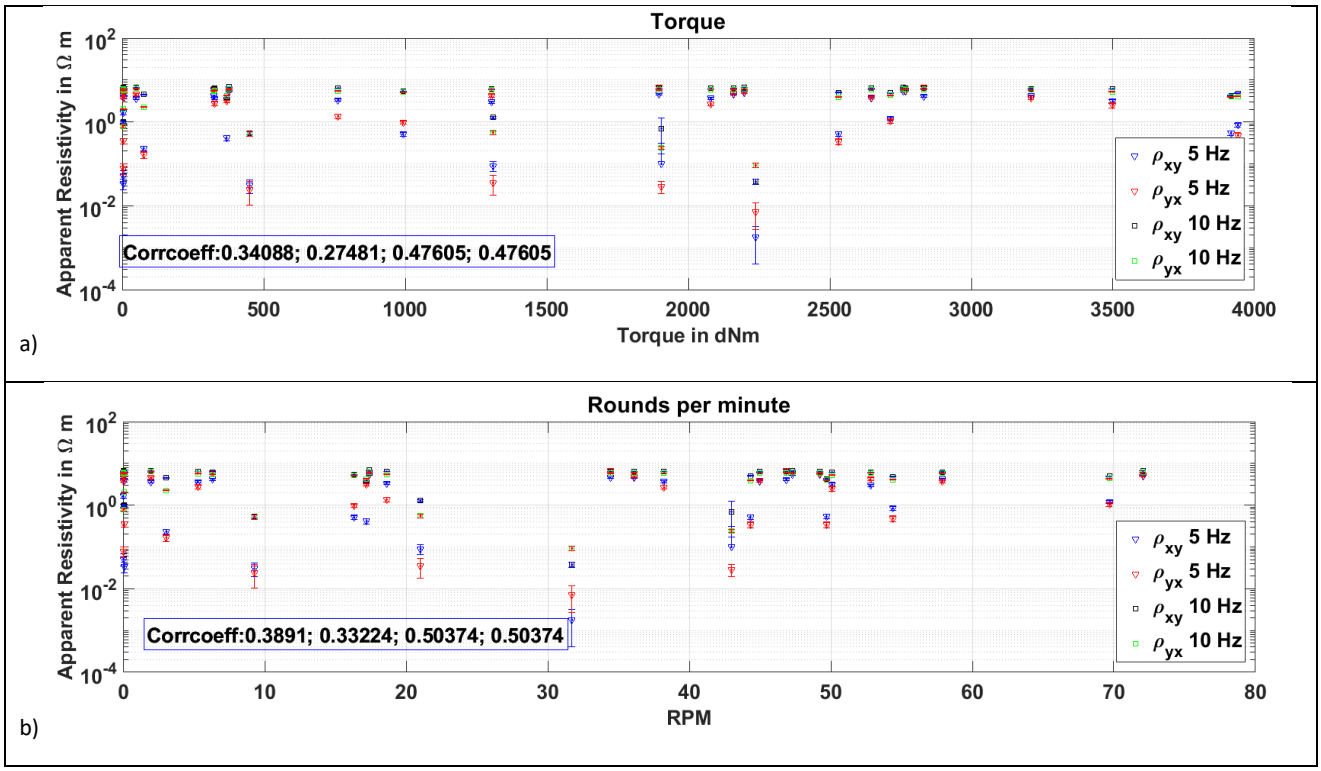

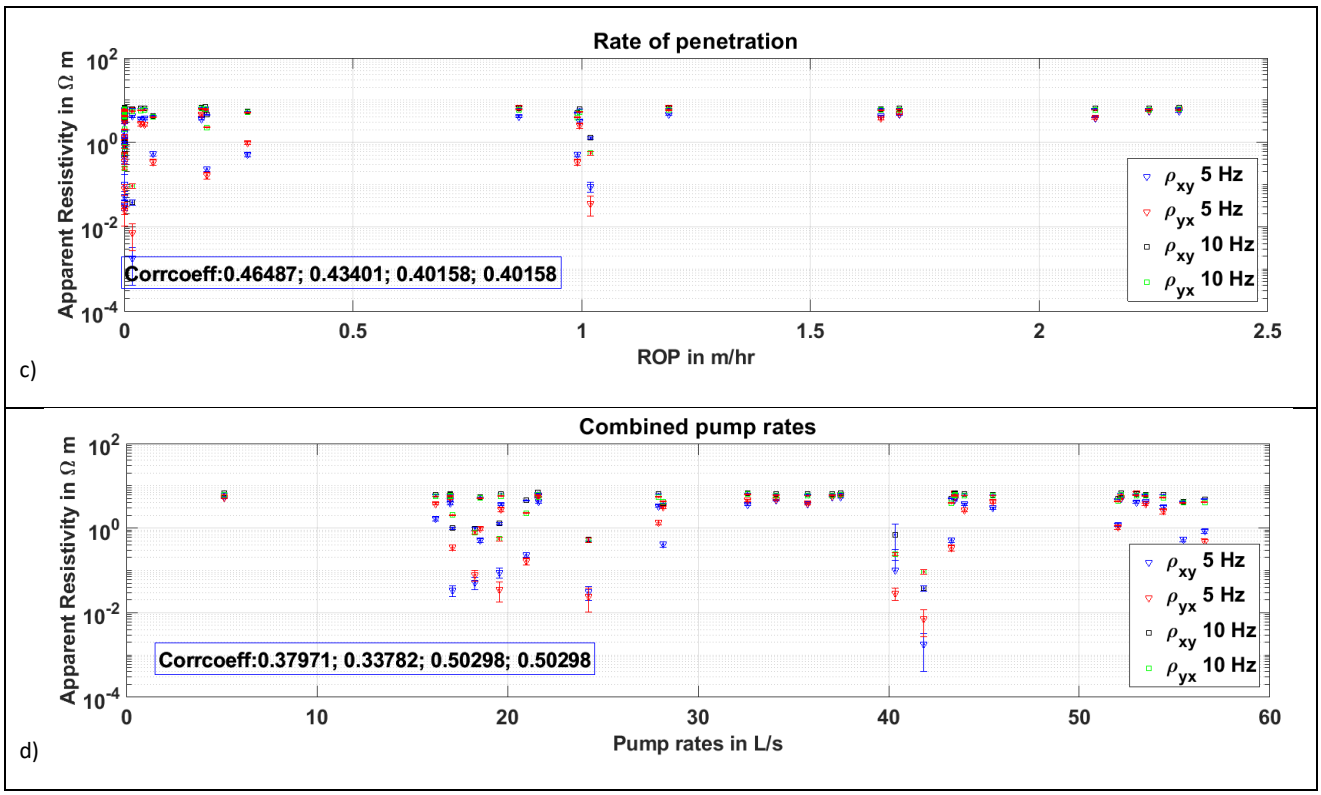

Figure 4.10: The correlation between apparent resistivity at 5 and 10 Hz for both polarizations XY and YX and the drilling parameters presented in Figure 4.9 for a) torque, b) number of rotations, c) rate of penetration, and d) the total pumping rate.

4.4 Single Site processing with data filtering

Since e.g. the 14 Hz noise (Figure 4.1) with a duration of about 60-90 s occurs approximately every half hour between November 30th and December 18th 2016, deletion of the noise from the data would result in a data loss of about 50-70 minutes per day. To better visualize the noise peaks in the spectrum, the data were decimated to lower frequency bands (128 Hz). Pre-filtering using notch filter for the respective bandwidths were applied to the 128. The results are presented in Figure 4.11. The spectra indicate a significant elimination of the 14 Hz noise signal and a clear reduction in amplitude is shown in the time series. However, a complete elimination of the peak is not obtained.

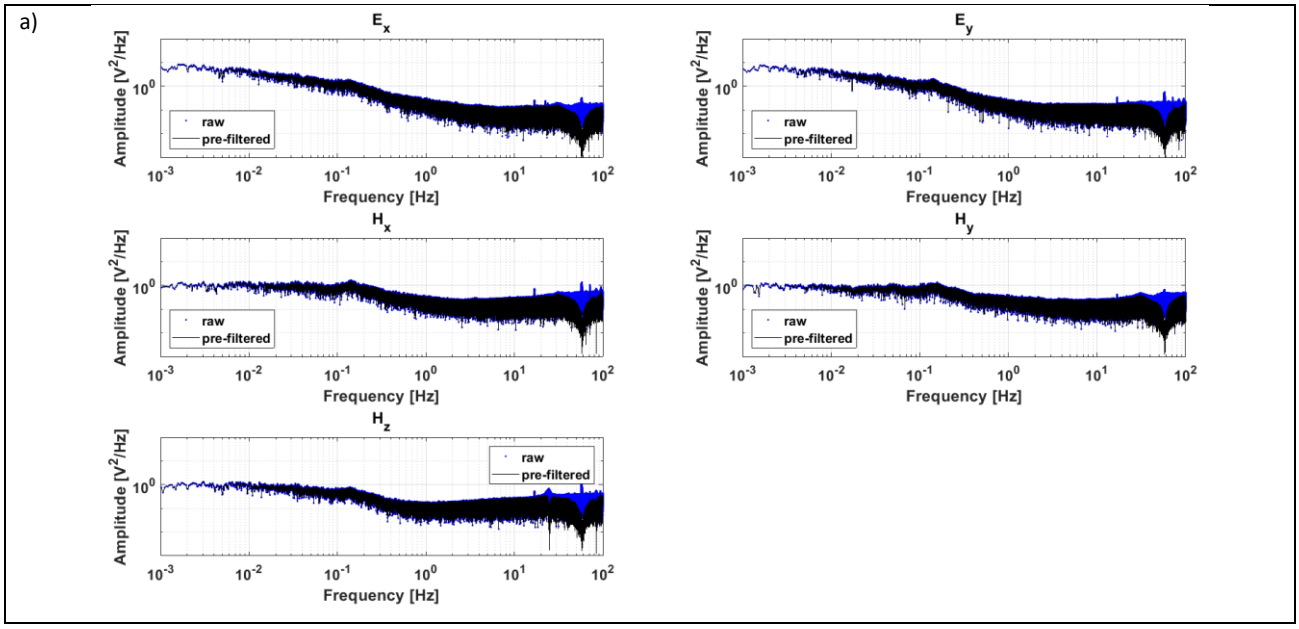

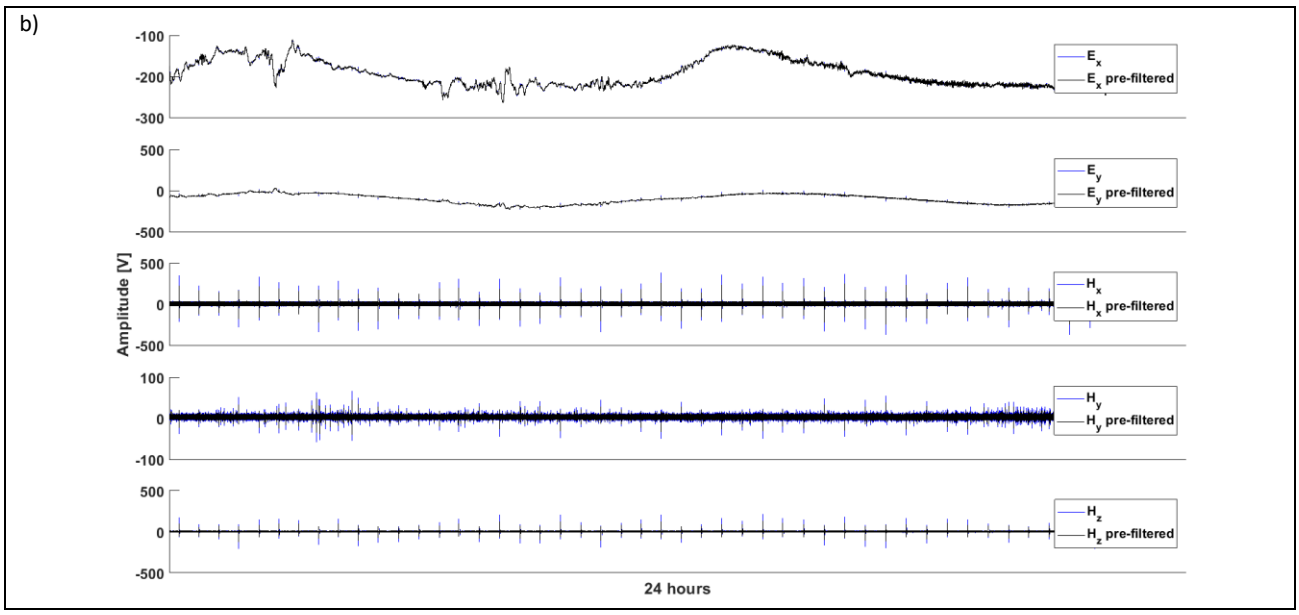

Figure 4.11 a) Comparison of a) noise spectra and b) time series of the measured (decimated to 128 Hz for frequencies < 1 Hz) and filtered data of the electric and magnetic components from December 11th, 2016 of GUN MT station.

Finally, the processed transfer functions are now composed of 512 Hz for the high frequency range down to 10 Hz and 128 Hz for the low frequencies > 1 Hz. Between 1 and 10 s (including the dead band), the sampling frequency with lower error bars is used.

5. DISCUSSION AND CONCLUSION

Due to the high frequency of the perturbations applied during drilling and reservoir engineering and the therefore presumed high frequency of changes in the electromagnetic field, in MT monitoring, conventional processing of MT data as applied in exploration with the aim to obtain smoothest distribution must be questioned in our case.

Here we demonstrated that low perturbations represented by low error bars in the transfer functions are not improved by remote referencing. The data uncertainties in the transfer functions were computed using the robust statistical Jackknife approach (Chave and Thomson 2004). In contrast, the changes in electric resistivity, which have been related to fluid injection in comparable studies (e.g. (Abdelfettah et al. 2018), appear as uncorrelated noise in the remote referenced processing. To eliminate only the uncorrelated noise that originates from operations at the surface, we propose to apply notch filters of the respective frequencies. In the case of high frequency signal an improvement of filtering is achieved by decimation of the sampling frequency prior to the filtering.

ACKNOWLEDGEMENTS

The DEEPEGS project has received funding from the European Union's HORIZON 2020 research and innovation program under grant agreement No 690771. We would like to thank P. Saillhac (EOST) for providing processing software in the framework of the Labex G-Eau-Thermie Profonde, which is co-funded by the French government under the program “Investissements d'Avenir”. Futhermore, we thank Albert Þorbergsson and Stefan Audunn Stefansson for surveying the MT stations. In addition, we would like to thank Anne Neska for her helpful input about this work. The Geophysical Instrument Pool Potsdam (GIPP) provided data from permanent magnetotelluric reference station. This work is partly supported through the Helmholtz-Portfolio project Geoenergy and the Helmholtz renewable energy program

PUBLICATION BIBLIOGRAPHY

Abdelfettah, Y.; Sailhac, P.; Larnier, H.; Matthey, P.-D.; Schill, E. (2018): Continuous and time-lapse magnetotelluric monitoring of low volume injection at Rittershoffen geothermal project, northern Alsace – France. In *Geothermics* 71, pp. 1–11. DOI: 10.1016/j.geothermics.2017.08.004.

Chave, Alan D.; Jones, Alan G.; Mackie, Randall; Rodi, William (2012): The Magnetotelluric Method. Cambridge: Cambridge University Press.

Chave, Alan D.; Thomson, David J. (2004): Bounded influence magnetotelluric response function estimation. In *Geophysical Journal International* 157 (3), pp. 988–1006. DOI: 10.1111/j.1365-246X.2004.02203.x.

CLARKE, J.; GAMBLE, T. D.; GOUBAU, W. M.; KOCH, R. H.; MIRACKY, R. F. (1983): REMOTE-REFERENCE MAGNETOTELLURICS. EQUIPMENT AND PROCEDURES*. In *Geophys Prospect* 31 (1), pp. 149–170. DOI: 10.1111/j.1365-2478.1983.tb01047.x.

Darnet, M.; Wawrzyniak, P.; Coppo, N.; Nielsson, S.; Schill, E.; Fridleifsson, G.Ó. (2018): Monitoring geothermal reservoir developments with the Controlled-Source Electro-Magnetic method — A calibration study on the Reykjanes geothermal field. In *Journal of Volcanology and Geothermal Research. DOI:* 10.1016/j.jvolgeores.2018.08.015.

Didana, Yohannes Lemma; Heinson, Graham; Thiel, Stephan; Krieger, Lars (2017): Magnetotelluric monitoring of permeability enhancement at enhanced geothermal system project. In *Geothermics* 66, pp. 23–38. DOI: 10.1016/j.geothermics.2016.11.005.

Friðleifsson, G.Ó.; Sigurdsson, Ó.; Þorbjörnsson, D.; Karlsdóttir, R.; Gíslason, Þ.; Albertsson, A.; Elders, W. A. (2014): Preparation for drilling well IDDP-2 at Reykjanes. In *Geothermics* 49, pp. 119–126. DOI: 10.1016/j.geothermics.2013.05.006.

Friðleifsson, Guðmundur Ómar; Elders, Wilfred A.; Zierenberg, Robert; Weisenberger, Tobias B.; Harðarson, Björn S.; Stefánsson, Ari et al. (2017): IDDP-2-Completion-websites-IDDP-DEEPEGS-5: Scientific Drilling, (23, 1-12.).

GAMBLE, T. D.; GOUBAU, W. M.; CLARKE, J. (1979): Magnetotellurics with a remote magnetic reference. In *GEOPHYSICS* 44 (1), pp. 53–68. DOI: 10.1190/1.1440923.

Peacock, J. R.; Thiel, S.; Reid, P.; Heinson, G. (2012): Magnetotelluric monitoring of a fluid injection. Example from an enhanced geothermal system. In *Geophys. Res. Lett.* 39 (18), p. 165. DOI: 10.1029/2012GL053080.

Peacock, Jared R.; Thiel, Stephan; Heinson, Graham S.; Reid, Peter (2013): Time-lapse magnetotelluric monitoring of an enhanced geothermal system. In *GEOPHYSICS* 78 (3), B121-B130. DOI: 10.1190/geo2012-0275.1.

Ritter, Oliver; Muñoz, G.; Weckmann, Ute; Klose, Reinhard; Rulff, Paula; Rettig, St. et al. (2015a): A Permanent Magnetotelluric Remote Reference Station in Wittstock, Germany.

Ritter, Oliver; Muñoz, Gerard; Weckmann, Ute; Klose, Reinhard; Rettig, Stefan; Schüler, Manfred et al. (2015b): Permanent Magnetotelluric Reference Station Wittstock, Germany. With assistance of Oliver Ritter, Gerard Muñoz, Ute Weckmann, Reinhard Klose, Stefan Rettig, Manfred Schüler et al.